Hindawi Publishing Corporation
Mathematical Problems in Engineering
Volume 2015, Article ID 253179, 10 pages
http://dx.doi.org/10.1155/2015/253179

Research Article

Computational Methods for Coupled Fluid-Structure-Electromagnetic Interaction Models with Applications to Biomechanics

Felix Mihai, Inja Youn, Igor Griva, and Padmanabhan Seshaiyer

Department of Mathematical Sciences, College of Science, George Mason University, 4400 University Drive, MS 3F2, Fairfax, VA 22030, USA

Correspondence should be addressed to Padmanabhan Seshaiyer; pseshaiy@gmu.edu

Received 29 August 2014; Accepted 15 November 2014

Academic Editor: Kim M. Liew

Multiphysics problems arise naturally in several engineering and medical applications which often require the solution to coupled processes, which is still a challenging problem in computational sciences and engineering. Some examples include blood flow through an arterial wall and magnetic targeted drug delivery systems. For these, geometric changes may lead to a transient phase in which the structure, flow field, and electromagnetic field interact in a highly nonlinear fashion. In this paper, we consider the computational modeling and simulation of a biomedical application, which concerns the fluid-structure-electromagnetic interaction in the magnetic targeted drug delivery process. Our study indicates that the strong magnetic fields, which aid in targeted drug delivery, can impact not only fluid (blood) circulation but also the displacement of arterial walls. A major contribution of this paper is modeling the interactions between these three components, which previously received little to no attention in the scientific and engineering community.

1. Introduction

In the last decade, the rapid development of computational science has provided new methodologies to solve complex multiphysics applications involving fluid-structure interaction to a variety of fields. These include solving applications involving blood flow interactions with the arterial wall to computational aeroelasticity of flexible wing micro-air vehicles to magnetohydrodynamic of liquid-metal cooled nuclear reactor to ferromagnetics with biological applications. In these applications, the challenge is to understand and develop algorithms that allow the structural deformation, the flow field, and temperature variations to interact in a highly nonlinear fashion.

Coupling these multiphysics with electromagnetic effects makes the associated computational model too complex. Not only is the nonlinearity in the geometry challenging but in many of these applications the material is nonlinear as well, which makes the problem even more complex. Direct numerical solution of the highly nonlinear equations governing even the most simplified two-dimensional models of such multiphysics interaction requires that all the unknown fields, such as fluid velocity, pressure, the magnetic and the electric field, the temperature field, and the domain shape, be determined as part of the solution, since neither is known a priori.

The past few decades, however, have seen significant advances in the development of finite element and domain decomposition methods. These have provided new algorithms for solving such large scale multiphysics simulations. There have been several methods that have been introduced in this regard and their performance has been analyzed for a variety of problems. One such technique is the mortar finite element method which has been shown to be stable mathematically and has been successfully applied to a variety of applications and references therein. The basic idea is to replace the strong continuity condition at the interfaces between the different subdomains modeling different

multiphysics by a weaker one to solve the problem in a coupled fashion. Such novel techniques provide hope for us to develop new faster and efficient algorithms to solve complex multiphysics applications. A variety of methods have been introduced including the level set methods [1], fictitious domain methods [2, 3], nonconforming hp finite element methods [4, 5], multilevel multigrid methods [6], and the immersed boundary methods [7]. While these methods help enhance our ability to understand complex processes, there is still a great need for efficient computational methods that cannot only help simulate physiologically realistic situations qualitatively but also analyze and study modeling of such processes quantitatively. Such multiphysics applications involve the interaction of various components, such as fluid with the structure, electromagnetics with the fluid, or fluid-structure interacting completely with electromagnetics.

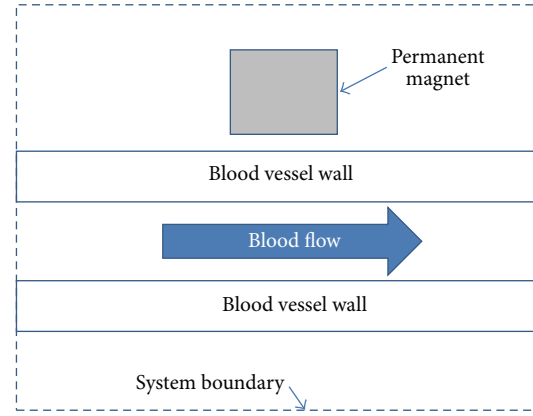

Figure 1: Electromagnetic fluid-structure interaction model.

1.1. Electromagnetic-Fluid Interaction. An important application involving interaction of electromagnetics with fluid which describes the behavior of electrically conducting fluid is very complex under a magnetic field, since the additional Lorentz force is caused by the interaction between velocity field and electromagnetic field. Understanding such coupled behavior not only helps us to create efficient algorithms but also applies to a variety of magnetohydrodynamic (MHD) applications. Due to its multidisciplinary applications, a solid understanding of the MHD is required. In this regard, the Hartmann flow has been studied extensively. The Hartmann flow is the steady flow of an electrically conducting fluid between two parallel walls, under the effect of a normal magnetic and electric field. A thorough understanding of such models for electromagnetic fluid interaction can help us in developing new techniques for complex problems such as magnetic drug targeting in cancer therapy. Such a model would involve ferrohydrodynamics of blood that helps to study external magnetic field and its interaction with blood flow containing a magnetic carrier substance. The analytic models would involve solving Maxwell's equations in conjunction with Navier-Stokes equations. While new models in this area are just starting to evolve, these often consider the structure to be fixed. There is a need to extend these models to include fluid-structure interaction with electromagnetics, which would be another focus of this work.

1.2. Proposed New Models. In this paper, we will develop a computational infrastructure for solving coupled fluid-structure interaction with electromagnetic and temperature effects. The rest of the work is organized as follows. Section 2 presents the models, methods, and background required to develop and solve the coupled multiphysics systems. In Section 3, we consider the model of a blood vessel, a permanent magnet, and surrounding tissue and air in two dimensions. We will consider both a nonmoving structure and a moving structure. The deformed structure provides a new geometry, where the Navier-Stokes equations are solved for the velocity and pressure fields in the bloodstream. A magnetic vector potential generated by the permanent magnet is calculated, which in turn creates a magnetic volume force that impacts the flow in the blood vessel. The flow field changes the displacement of the structure, and the problem is solved once again for the new geometry. The proposed models are validated against benchmark applications numerically. Section 4 presents conclusion and a discussion of the results. Future work on the proposed problems is also presented.

A magnetically targeted drug delivery system [8] is based on magnetic particles under the action of an external magnetic field. This is becoming an increasingly effective approach in drug therapy. As this field has evolved in the last decade, lots of scientific interest led to this inquiry into efficient computational models that simulate this experimental process [9]. Our study indicates that the strong magnetic fields which aid in targeted drug delivery can impact not only fluid (blood) circulation but also the displacement of arterial walls. Thus, it is important to have a model, which includes the interactions between fluid, structure, and magnetic field in order to study and optimize drug delivery.

In this section, we will present a model that describes the interaction between these three components, which previously received little to no attention in the scientific community. To develop an electromagnetic fluid-structure interaction, we incorporate the effects of the electromagnetic field into a fluid-structure model. Gaining a thorough understanding of such a coupled model can help us to understand the efficacy of magnetic nanoparticle-based drug delivery for diseases such as cancer as has been proposed by various researchers [10, 11]. There is significant evidence that indicates a need for more promising models which overcome current limitations and improve magnetic targeting technique.

2. Mathematical Model and Governing Equations

The model we consider is a blood vessel with a permanent magnet near its surface, as illustrated in Figure 1. For simplicity of presentation, we consider a computational model that comprises three components. Let the computational domain $\Omega \subset \mathbf{R}^2$ be an open set with global system boundary Γ. Let Ω be decomposed into the four disjoint open sets, a fluid subdomain Ω_f denoted by blood flow, two solid

subdomains Ω_s^i, $i = 1, 2$ (blood vessel walls) with respective boundaries Γ_f and Γ_s, and one electromagnetic domain Ω_m (permanent magnet). Let Γ_I^j, $i = 1, 2, 3, 4$ be the interface between the solid, fluid, and electromagnetic domains. The structural domain consists of two symmetric arterial vessel walls denoted by Ω_s^1 and Ω_s^2. The electromagnetic domain consists of a permanent magnet of dimensions $10\,\mu\text{m} \times 40\,\mu\text{m}$ placed in free space. The arterial wall describes a structural mechanism that interacts with the flow dynamics of blood which in turn is impacted by a permanent magnet, which is described next.

For this, we use Maxwell's equation for the magnetostatic case (the field quantities do not vary with time) that relates the magnetic field intensity $\mathbf{H}$ and the electric current density $\mathbf{J}$ [12]:

$$\begin{aligned} \nabla \times \mathbf{H} &= \mathbf{J}, \\ \nabla \cdot \mathbf{J} &= 0. \end{aligned} \tag{1}$$

The constitutive relations between $\mathbf{B}$ and $\mathbf{H}$ depend on the domain [12, 13]:

$$\mathbf{B} = \begin{cases} \mu_0 \mu_{r,\text{mag}} \mathbf{H} + \mathbf{B}_{\text{rem}} & \text{for the permanent magnet} \\ \mu_0 \left(\mathbf{H} + \mathbf{M}_{ff}(\mathbf{H}) \right) & \text{for the blood stream} \\ \mu_0 \mathbf{H} & \text{for the tissue and air,} \end{cases} \tag{2}$$

where μ_0 is the magnetic permeability of vacuum (V·s/(A·m)), $\mu_{r,\text{mag}}$ is the relative magnetic permeability of the permanent magnet (dimensionless), $\mathbf{B}_{\text{rem}}$ is the remanent magnetic flux (A/m), and $\mathbf{M}_{ff}$ is the magnetization vector in the blood stream (A/m), which is a function of the magnetic field, $\mathbf{H}$. By defining a magnetic vector potential $\mathbf{A}$ such that

$$\mathbf{B} = \nabla \times \mathbf{A}, \quad \text{with } \nabla \cdot \mathbf{A} = 0, \tag{3}$$

we get

$$\nabla \times \left(\frac{1}{\mu} \nabla \times \mathbf{A} - \mathbf{M} \right) = \mathbf{J}. \tag{4}$$

Assuming no perpendicular currents, we can simplify to a 2D problem and reduce this equation to

$$\nabla \times \left(\frac{1}{\mu_0} \nabla \times \mathbf{A} - \mathbf{M} \right) = \mathbf{0}. \tag{5}$$

This assumes that the magnetic vector potential has a nonzero component only perpendicularly to the plane, which is $\mathbf{A} = (0, 0, A_z)$. The induced magnetization $\mathbf{M}_{ff}(x, y) = (M_{ffx}, M_{ffy})$ is characterized by [14–17]

$$\begin{aligned} \mathbf{M}_x &= \alpha \arctan\left(\frac{\beta}{\mu_0} \frac{\partial A_z}{\partial y} \right), \\ \mathbf{M}_y &= \alpha \arctan\left(\frac{\beta}{\mu_0} \frac{\partial A_z}{\partial x} \right). \end{aligned} \tag{6}$$

To capture the magnetic fields of interest we can linearize these expressions to obtain

$$\mathbf{M}_x = \frac{\chi}{\mu_0} \frac{\partial A_z}{\partial y}, \qquad \mathbf{M}_y = \frac{\chi}{\mu_0} \frac{\partial A_z}{\partial x}, \tag{7}$$

where $\chi = \alpha\beta$ is the magnetic susceptibility. This magnetic field induces a body force on the fluid. With the assumption that the magnetic nanoparticles in the fluid do not interact, the magnetic force $\mathbf{F} = (F_x, F_y)$ on the ferrofluid for relatively weak fields is given by [16]

$$\mathbf{F} = |\mathbf{M}| \nabla |\mathbf{H}|. \tag{8}$$

Substituting (2) and (3) in (8) leads to the expression

$$\begin{aligned} F_x &= k_{ff} \frac{\chi}{\mu_0 \mu_r^2} \left(\frac{\partial A_z}{\partial x} \frac{\partial^2 A_z}{\partial x^2} + \frac{\partial A_z}{\partial y} \frac{\partial^2 A_z}{\partial x \partial y} \right), \\ F_y &= k_{ff} \frac{\chi}{\mu_0 \mu_r^2} \left(\frac{\partial A_z}{\partial x} \frac{\partial^2 A_z}{\partial x \partial y} + \frac{\partial A_z}{\partial y} \frac{\partial^2 A_z}{\partial y^2} \right), \end{aligned} \tag{9}$$

where k_{ff} is the fraction of the fluid which is ferrofluid. The vector $F_f = (F_x, F_y)$ is the volume force, which is input for the Navier-Stokes equations in the next subsection.

2.1. Modeling the Unsteady Blood Flow. We model the fluid domain for the blood flow via the unsteady Navier-Stokes equations for an incompressible, isothermal fluid flow written in nonconservative form as

$$\begin{aligned} \rho_f \frac{\partial u_f}{\partial t} + \rho_f \left(u_f \cdot \nabla \right) u_f + \nabla p &= \nabla \cdot \tau_f + F_f, \\ \rho_f \nabla \cdot u_f &= 0, \end{aligned} \tag{10}$$

where u_f is the velocity, ρ_f is the density, p is the pressure, and F_f is the body forces. The viscous stress tensor is $\tau(u_f) = 2\eta D(u_f)$, where η is the dynamic viscosity and the deformation tensor is

$$D\left(u_f\right) = \mu_s \left(\frac{\nabla u_f + \left(\nabla u_f \right)^T}{2} \right). \tag{11}$$

The fluid equations are subject to the boundary conditions:

$$\begin{aligned} u_f &= u_{\text{wall}}, \quad x \in \Gamma_I^j, \quad j = 2, 3 \\ \tau_f \cdot n &= t \cdot n, \quad x \in \Gamma_N, \\ u_f &= \frac{\partial d_s}{\partial t} \qquad x \in \Gamma_I^j, \quad j = 2, 3, \end{aligned} \tag{12}$$

where $t = -pI + 2D(u_f)$ is the prescribed tractions on the Neumann part of the boundary with n being the outward unit normal vector to the boundary surface of the fluid. Conditions of displacement compatibility and force equilibrium along the structure-fluid interface are enforced. In order to solve a fluid-structure interaction problem in a coupled fashion we employ an arbitrary Lagrangian-Eulerian (ALE) formulation where the characterizing velocity is no longer the material velocity u_f, but a grid velocity $\widehat{u}_f$. This allows us to replace the material velocity u_f in (10) with the convective

velocity $c = u_f - \widehat{u}_f$ [5]. The weak variational formulation of the fluid problem then becomes

$$\begin{aligned}&\int_{\Omega_f} \tau_f \cdot \nabla\phi \; d\Omega_f \\ &\quad = \int_{\Omega_f} F \cdot \phi \; d\Omega_f + \int_{\Gamma_f} t \cdot \phi \; d\Gamma \\ &\qquad + \int_{\Omega_f} \rho_f \frac{\partial u}{\partial t} \cdot \phi \; d\Omega_f + \int_{\Omega_f} \rho_f \left(c \cdot \nabla\right) u_f \cdot \phi \; d\Omega_f, \\ &\qquad \int_{\Omega_f} q \nabla \cdot u \; d\Omega_f = 0.\end{aligned} \tag{13}$$

2.2. Modeling the Structure Equations. The structural domains for the blood vessel walls consist of the arterial vessel walls denoted by Ω_s^1, Ω_s^2. They are modeled via the following equation:

$$\rho_s \frac{\partial^2 d_s}{\partial t^2} = \nabla \cdot \tau_s + F_s, \tag{14}$$

where d_s is the structure displacement, ρ_s is the structure density, τ_s is the solid stress tensor, and $\partial^2 d_s/\partial t^2$ is the local acceleration of the structure. This is solved with the boundary conditions:

$$\begin{aligned} d_s &= d_s^D \quad x \in \Gamma_S^D, \\ \tau_s \cdot n_s &= t_s \quad x \in \Gamma_S^N, \\ \tau_s \cdot n_s &= -\tau \cdot n + t_S^I \quad x \in \Gamma_I^j \quad j = 2, 3. \end{aligned} \tag{15}$$

Here Γ_S^D and Γ_S^N are the respective parts of the structural boundary where the Dirichlet and Neumann boundary conditions are prescribed. Also, t_S are the applied tractions on Γ_S^N and t_S^I are the externally applied tractions to the interface boundaries Γ_I^j, $j = 1, 2, 3, 4$. The unit outward normal vector to the boundary surface of the structure is n_s. The stresses are computed using the constitutive relation described next. Equations (15) enforce the equilibrium of the traction between the fluid and the structure on the respective fluid-structure interfaces. The total strain tensor for a typical geometrically nonlinear model is written in terms of displacement gradients:

$$\varepsilon = \frac{1}{2}\left(\nabla d_s + \nabla d_s^T + \nabla d_s \nabla d_s^T\right). \tag{16}$$

For small deformations, the last term on the right hand side is omitted to obtain a geometrically linear model. Since the objective of this section is to investigate the influence of electromagnetic effects on fluid-structure interaction models, we will consider a geometrically linear model combined with a linear constitutive law. The solid stress tensor τ_s is given in terms of the second Piola-Kirchoff stress S:

$$\tau_s = \left(S \cdot \left(I + \nabla d_s\right)\right). \tag{17}$$

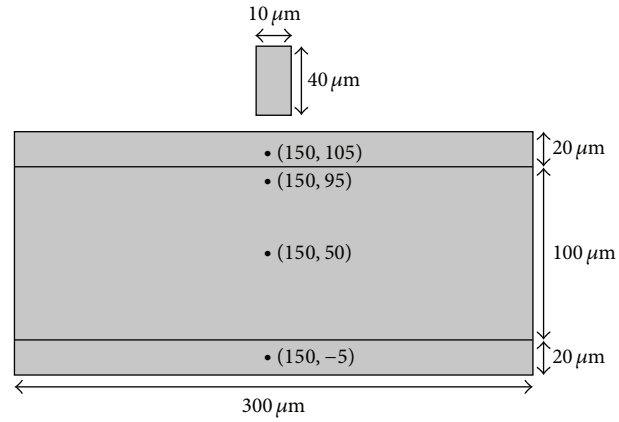

Figure 2: Domain and points of interest.

For the linear material model, we employ the following constitute law relating the stress tensor to the strain tensor:

$$S = S_0 + C : \varepsilon, \tag{18}$$

where C is the 4th order elasticity tensor and ":" stands for the double-dot tensor product. S_0 and ε_0 are initial stresses and strains, respectively. The weak variational form of the structural equations then becomes the following: find the structure displacement u_s such that

$$\begin{aligned}&\int_{\Omega_f} \tau_s \cdot \varepsilon_s \; d\Omega_s \\ &\quad = \int_{\Omega_f} F_s \cdot \phi_s \; d\Omega_s + \int_{\Gamma_S^N} t_s \cdot \phi_s \; d\Gamma \\ &\qquad - \int_{\Omega_f} \rho_s \frac{\partial^2 d_s}{\partial t^2} \cdot \phi_s \; d\Omega_s - \int_{\Gamma_I} \left(t_S^I - \tau_f \cdot n\right) \cdot \phi_s \; d\Gamma.\end{aligned} \tag{19}$$

3. Numerical Results

In this section, we present the numerical results for the electromagnetic-fluid-structure interaction model problem presented in this section. To understand the effects of the coupling between electromagnetic field and fluid-structure interaction models better, we first consider the interaction with a rigid structure, which is often employed in the most research problems that are only interested in studying the electromagnetic-fluid interaction. The computational domain (see Figure 2) represents a blood vessel that is 300 micrometers long and 100 micrometers in diameter, with walls 20 micrometers in thickness. All the results presented are for three magnetic fields: 0 T (no magnetic field), 0.5 T, and 1 T. The structure model we consider is linear (MLGL), which was introduced in Section 2.

3.1. Coupled Interaction with Rigid Structure. Figures 3(a), 4(a), and 5(a) illustrate the influence of the magnetic field on the interaction. These figures show the surface von Mises

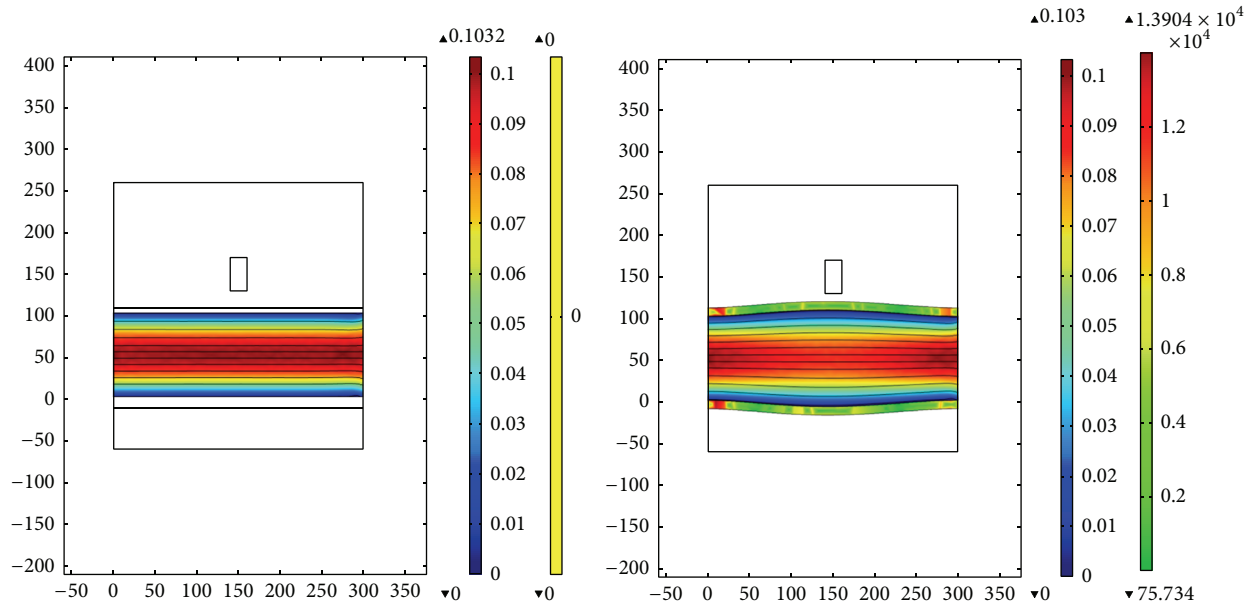

(a) Nonmoving structure (b) Moving structure

FIGURE 3: Surface von Mises stress with streamlines of spatial velocity field and magnetic field for $\mathbf{B}_{\text{rem}} = 0\,\text{T}$ at $t = 0.215$. Time = 0.215, surface: von Mises stress (N/m^2), surface: velocity magnitude (m/s), and streamline: velocity field (spatial).

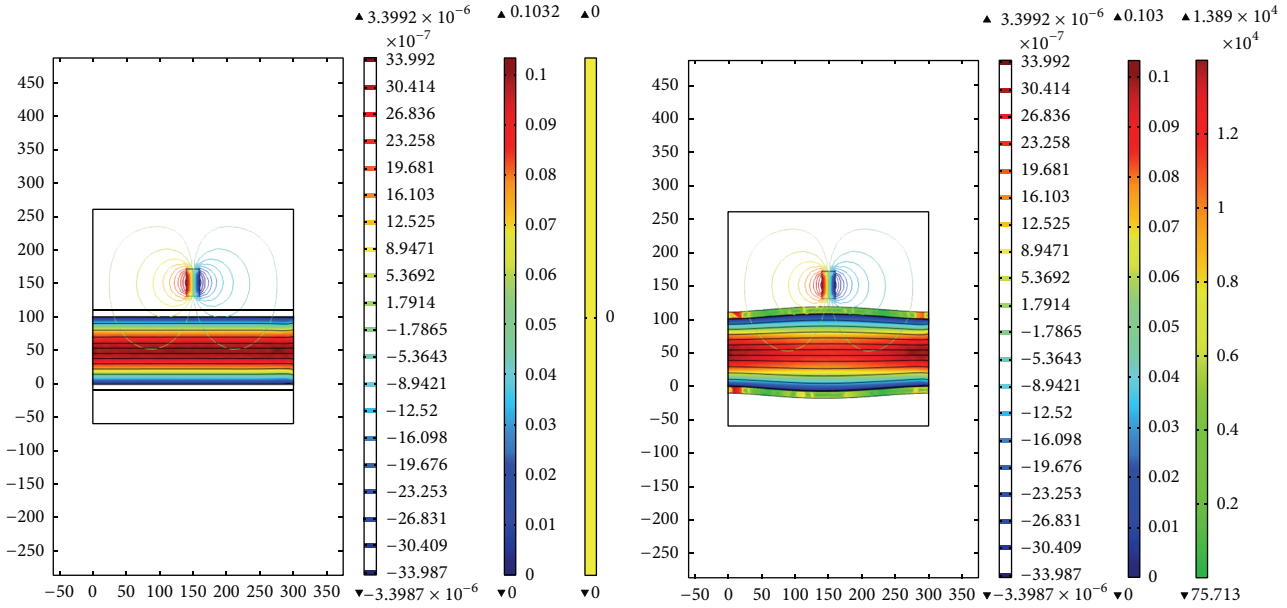

(a) Nonmoving structure (b) Moving structure

FIGURE 4: Surface von Mises stress with streamlines of spatial velocity field and magnetic field for $\mathbf{B}_{\text{rem}} = 0.5\,\text{T}$ at $t = 0.215$. Time = 0.215, surface: von Mises stress (N/m^2), surface: velocity magnitude (m/s), contour: magnetic vector potential, z component (Wb/m), and streamline: velocity field (spatial).

stress along with streamlines of spatial velocity field and the z-component of the magnetic vector potential. While there is no significant impact of increasing the magnetic field on the velocity profile in each of the graphs in Figures 3(a), 4(a), and 5(a), the impact on the magnetic vector potential is as expected. As it can be seen, the z-component of the magnetic potential doubles when magnetic field doubles.

Figures 6(a), 7(a), and 8(a) compare the effect of varying the magnetic field on the surface pressure. Unlike the impact on the velocity profile, these figures suggest that the surface

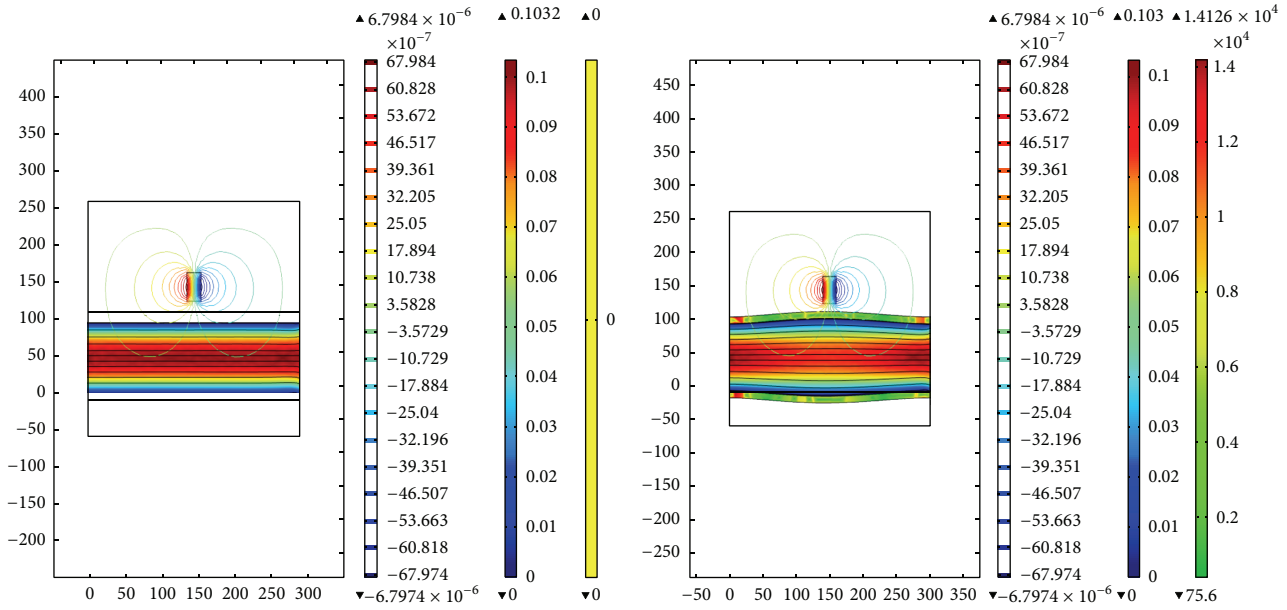

(a) Nonmoving structure (b) Moving structure

FIGURE 5: Surface von Mises stress with streamlines of spatial velocity field and magnetic field for $\mathbf{B}_{\text{rem}} = 1$ T at $t = 0.215$. Time = 0.215, surface: von Mises stress (N/m^2), surface: velocity magnitude (m/s), contour: magnetic vector potential, z component (Wb/m), and streamline: velocity field (spatial).

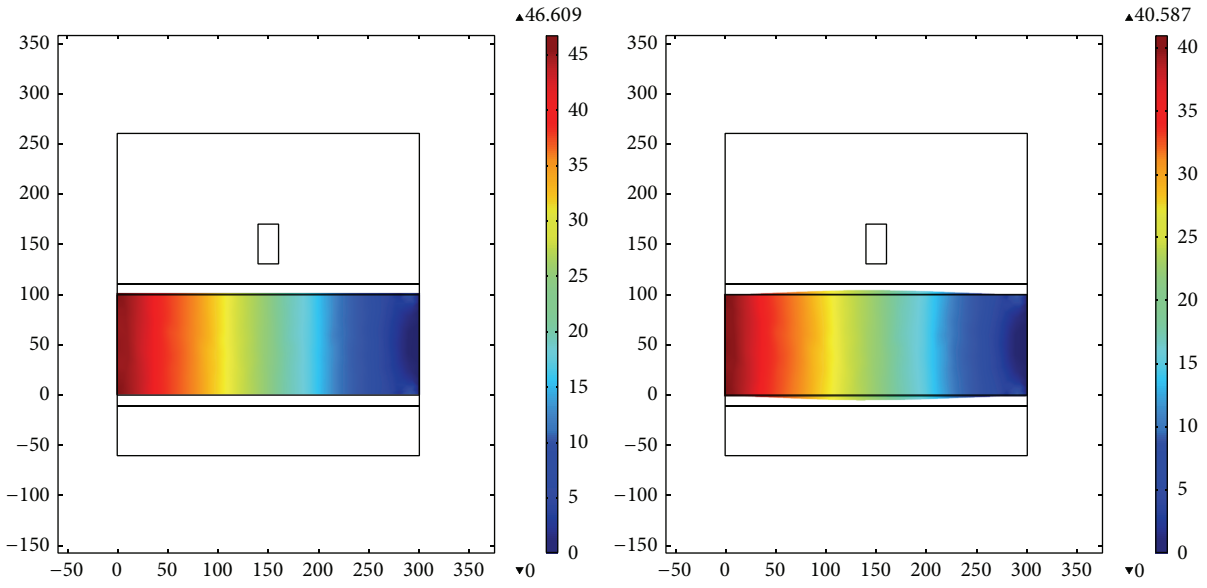

(a) Nonmoving structure (b) Moving structure

FIGURE 6: Pressure for $\mathbf{B}_{\text{rem}} = 0$ T shown at $t = 4$. Time = 4; surface: pressure (Pa).

pressure is impacted by increasing the magnetic field and the doubling effect is also seen as expected.

3.2. Coupled Interaction with Moving Structure. Next, we consider the benchmark problem presented with the structure moving. For this, we employ the ALE formulation for the fluid-structure interaction as described in Section 2. We notice from Figures 3(b), 4(b), and 5(b) that, at $t = 0.215$ (when the fluid velocity has maximum value), the structure and the flow pattern are not very much impacted by the magnet. For the maximum studied magnetic field of 1 T, the arterial wall is slightly bent towards the magnet. For even larger magnetic fields not shown in the picture (the order of magnetic field of 5 T), the magnet intersects with the arterial wall.

Even though we have not seen a big difference in structural deformation and fluid flow for our study case, the

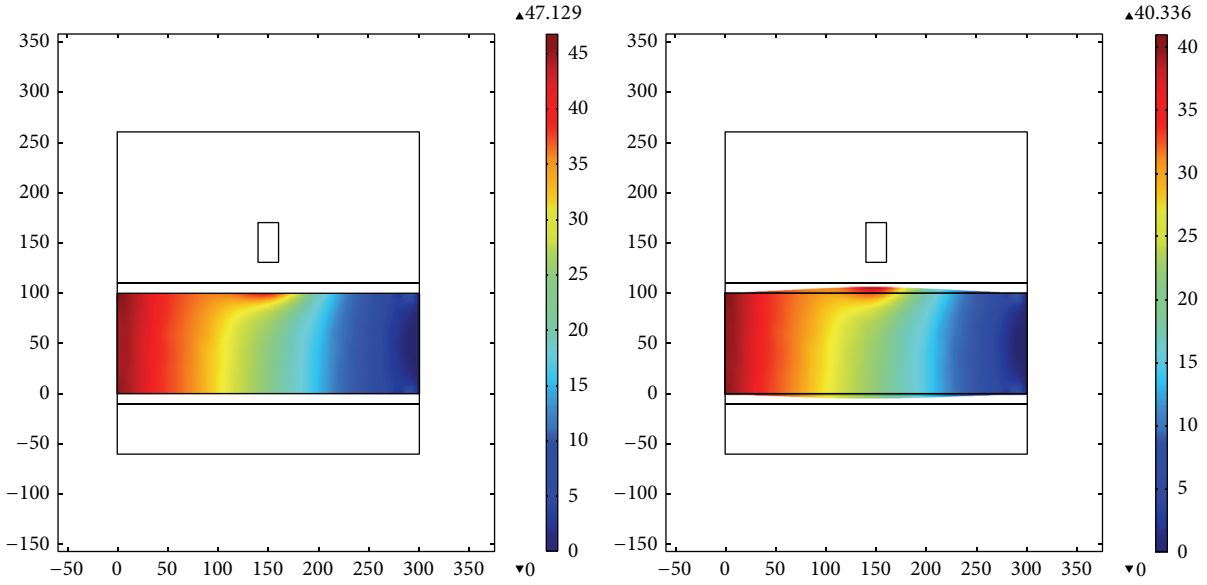

(a) Nonmoving structure (b) Moving structure

FIGURE 7: Pressure for $\mathbf{B}_{\text{rem}} = 0.5$ T shown at $t = 4$. Time = 4; surface: pressure (Pa).

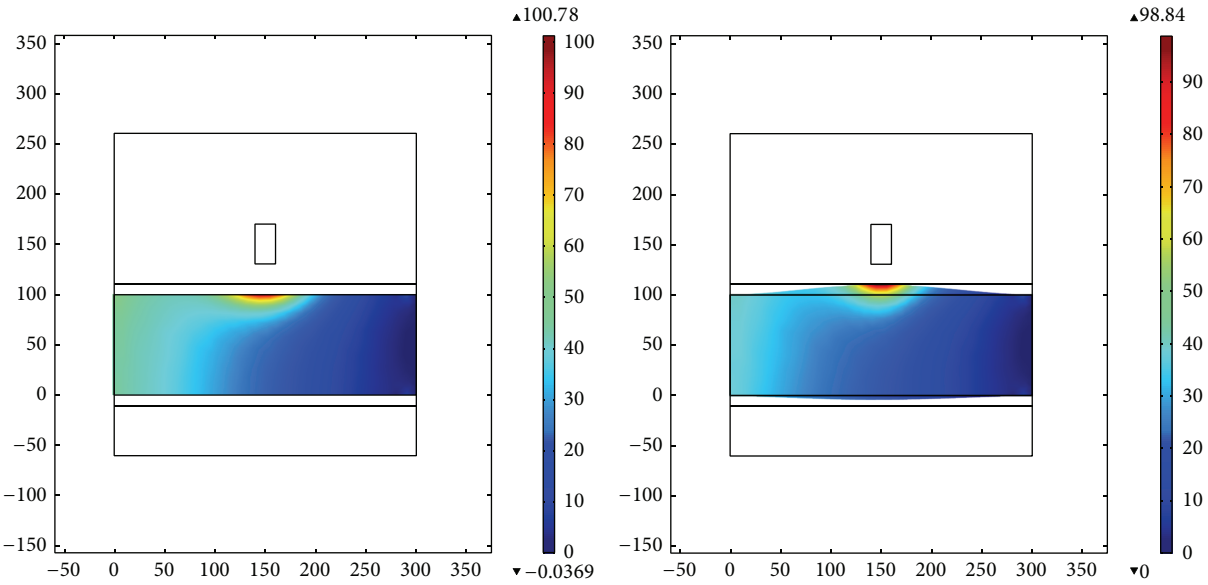

(a) Nonmoving structure (b) Moving structure

FIGURE 8: Pressure for $\mathbf{B}_{\text{rem}} = 1$ T shown at $t = 4$. Time = 4; surface: pressure (Pa).

fluid pressure is entirely different between two considered magnetic fields (see Figures 6(b), 7(b), and 8(b)). If for $\mathbf{B}_{\text{rem}} = 0$ T the pressure is completely symmetric with respect to the x-axis, the pressure around the magnet increases when magnetization is 0.5 T and becomes more than double the maximum pressure in the rest of the fluid when $\mathbf{B}_{\text{rem}} = 1$ T.

Another experiment we perform is to measure the velocity profile and displacement of two specific points. From Figures 9 and 10, we notice that, as expected, the velocity and pressure decrease at the center and increase around the boundaries when the structure is moving, mainly because of the dilatation of the structure. While the pressure in the center is not affected much by the presence or absence of magnetic field, near the magnet the pressure is steadily increasing with the time.

For the measured displacement, we notice in Figure 11 that the wall towards the magnet is getting closer to the magnet because of the increasing pressure, while the other wall is virtually unaffected by the presence of the magnetic field.

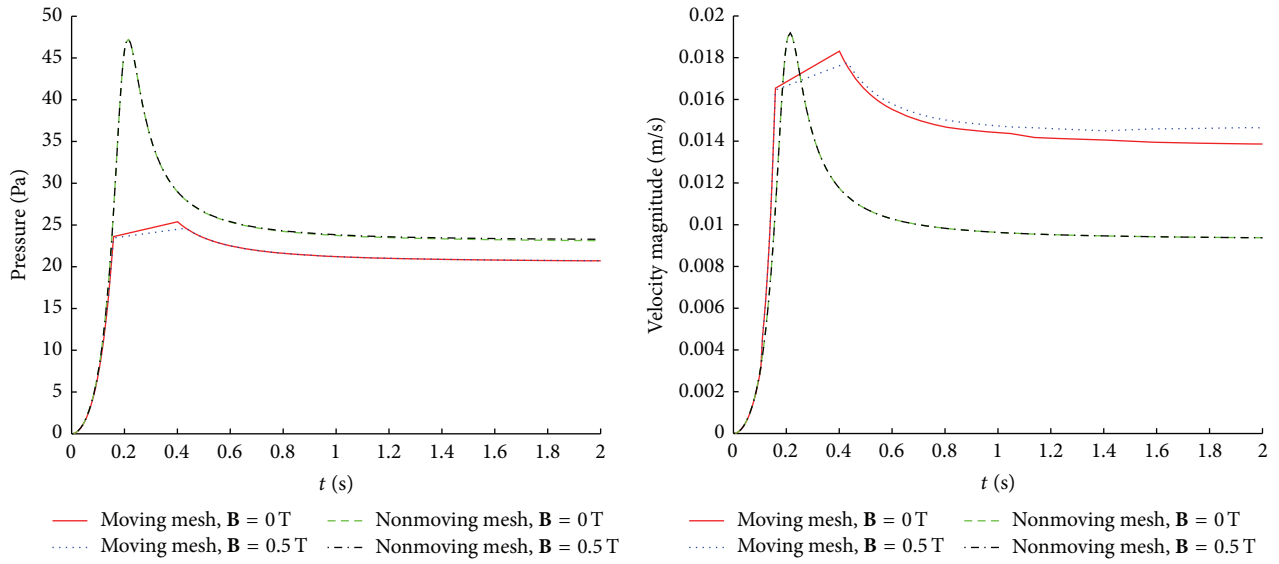

(a) Velocity profile for coordinates (150, 50)

(b) Velocity profile for coordinates (150, 95)

Figure 9: Velocity for a center and edge point inside the fluid.

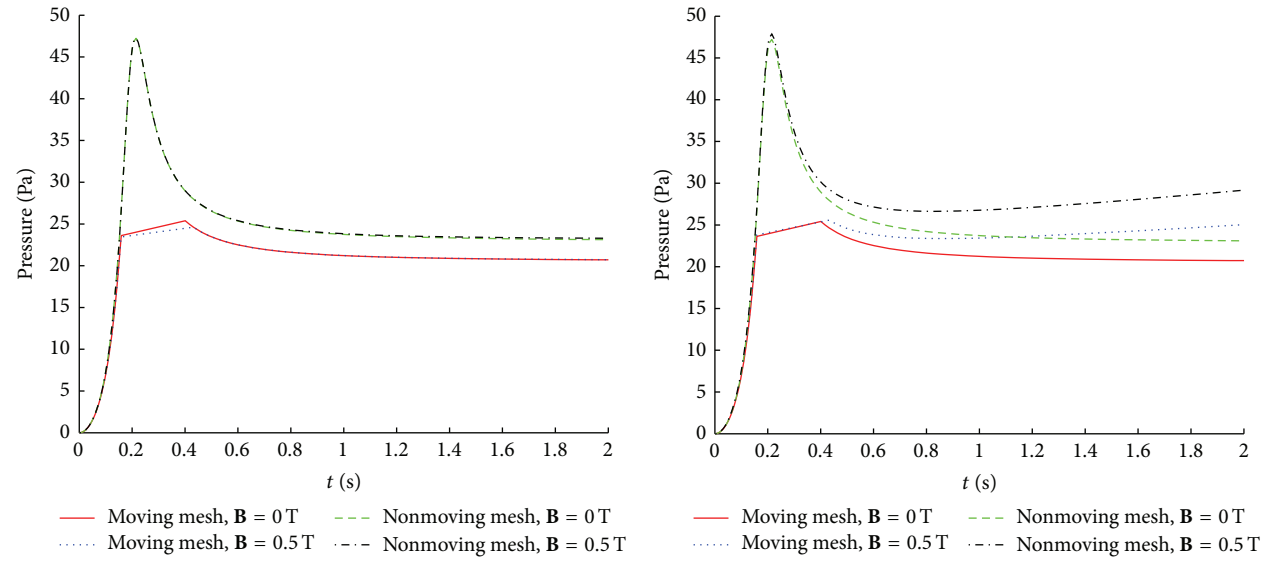

(a) Pressure profile for coordinates (150, 50)

(b) Pressure profile for coordinates (150, 95)

Figure 10: Pressure for a center and edge point inside the fluid.

4. Conclusion

In this work, we presented the computational modeling and simulation of coupled multiphysics applications. These included a variety of processes such as fluid dynamics, structural mechanics, and electromagnetic interaction that impacted the behavior of the physical system in a coupled way. Specifically, this work considered the research question of "how does incorporating electromagnetic field into fluid-structure interaction models influence the fluid flow and structural deformation?" In answering this question, this work led to the development of a two-dimensional multiphysics problem involving electromagnetics coupled with fluid-structure interaction.

In order to answer this research question, we first presented the mathematical background and simulation of the interaction between fluid, structure, and magnetic field. The motivation of this came from researching models for targeted drug delivery for delivering drugs in human body, to increase the concentration of the drug in the target area. For example, the chemotherapy drug dosage is limited by the negative impact on the drugs on the healthy cells. By delivering the

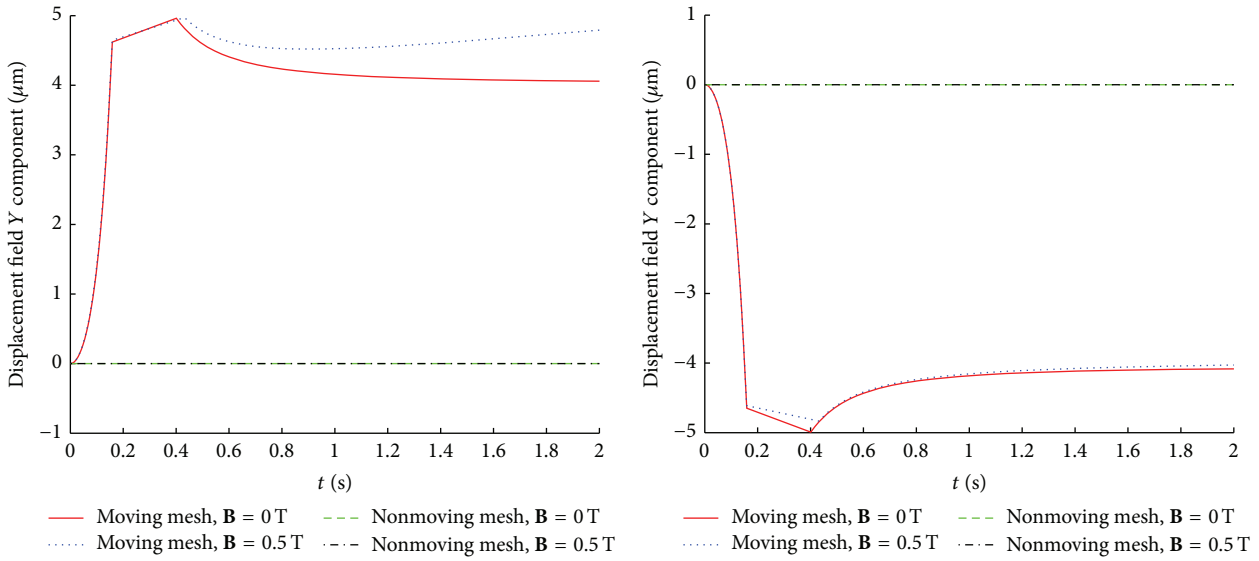

(a) y-displacement for coordinates (150, 105)

(b) y-displacement for coordinates (150, −5)

FIGURE 11: y-displacement of two points.

drugs with high accuracy and maximum concentration to specific areas of the body, it is possible to increase local dosage of the drug on the tumor, with lower concentration in the rest of the body. The drug effectiveness is increased while the side effects are reduced. Other examples of the applications of magnetic drug targeting are treatment of cardiovascular conditions, such as stenosis and thrombosis. Thus, it is important to model not only the blood circulation but also the deformation of the blood vessel, in order to improve the accuracy which is the focus of the second problem in this thesis. In particular, it is important to have an accurate model of the interaction between the three components for optimizing the shape, size, and magnetic power, in order to deliver the drugs efficiently in the desired place and minimize the side effects. Our results from this work clearly indicate the importance of the magnetic field to be coupled with a fluid-structure interaction model. More importantly, the results suggest the importance of using moving walls versus nonmoving walls in this coupled electromagnetic fluid-structure interaction.

While this work provided a lot of insight into the importance of electromagnetic effects in fluid-structure interaction, there is scope to enhance this work by considering effects of non-Newtonian rheological properties incorporated along with the extension to materially and geometrically nonlinear models. In the last two decades, collagenous soft tissues have been found to exhibit viscoelastic behavior, which includes time-dependent creep and stress relaxation, rate-dependence, and hysteresis in a loading cycle. As suggested in [18], this hysteresis is less sensitive than the stiffness to the loading rate, and this phenomenon is generally found in soft tissues and elastomers [18]. One of the future directions would be to extend the structural mechanics module to incorporate viscoelasticity and then study the influence of this on our models. The computational models in this work included two-dimensional models for simplicity, but our models can be naturally extended to three dimensions. With increasing the size of the problem comes the need for more computational resources. There is intensive work that is evolving in the area of domain decomposition that helps to address how to solve coupled multiphysics problems efficiently. So as the problem dimension becomes bigger, one must also resort to domain decomposition type approaches which can then open up more venues on parallelization of the algorithms that have been developed.

Conflict of Interests

The authors declare that there is no conflict of interests regarding the publication of this paper.

Acknowledgment

The authors wish to thank the STEM Accelerator Program in the College of Science at George Mason University for supporting this project in part to help promote scientific development for high school students and undergraduate and graduate students to learn about multidisciplinary research in STEM.

References

[1] Y. C. Chang, T. Y. Hou, B. Merriman, and S. Osher, "A level set formulation of Eulerian interface capturing methods for incompressible fluid flows," *Journal of Computational Physics*, vol. 124, no. 2, pp. 449–464, 1996.

[2] F. P. Baaijens, "A fictitious domain/mortar element method for fluid-structure interaction," *International Journal for Numerical Methods in Fluids*, vol. 35, no. 7, pp. 743–761, 2001.

[3] R. Glowinski, T. W. Pan, T. I. Hesla, D. D. Joseph, and J. Périaux, "A fictitious domain approach to the direct numerical simulation of incompressible viscous flow past moving rigid bodies: application to particulate flow," *Journal of Computational Physics*, vol. 169, no. 2, pp. 363–426, 2001.

[4] P. Seshaiyer, "Stability and convergence of nonconforming *hp* finite-element methods," *Computers & Mathematics with Applications*, vol. 46, no. 1, pp. 165–182, 2003.

[5] E. W. Swim and P. Seshaiyer, "A nonconforming finite element method for fluid-structure interaction problems," *Computer Methods in Applied Mechanics and Engineering*, vol. 195, no. 17, pp. 2088–2099, 2006.

[6] E. Aulisa, A. Cervone, S. Manservisi, and P. Seshaiyer, "A multilevel domain decomposition approach for studying coupled flow applications," *Communications in Computational Physics*, vol. 6, no. 2, pp. 319–341, 2009.

[7] C. S. Peskin, "Numerical analysis of blood flow in the heart," *Journal of Computational Physics*, vol. 25, no. 3, pp. 220–252, 1977.

[8] A. O. Mulyar, *Magnetically Targeted Drug Delivery System*, GRIN Verlag, 2010.

[9] A. D. Grief and G. Richardson, "Mathematical modelling of magnetically targeted drug delivery," *Journal of Magnetism and Magnetic Materials*, vol. 293, no. 1, pp. 455–463, 2005.

[10] J. Dobson, "Magnetic nanoparticles for drug delivery," *Drug Development Research*, vol. 67, no. 1, pp. 55–60, 2006.

[11] S.-I. Takeda, F. Mishima, S. Fujimoto, Y. Izumi, and S. Nishijima, "Development of magnetically targeted drug delivery system using superconducting magnet," *Journal of Magnetism and Magnetic Materials*, vol. 311, no. 1, pp. 367–371, 2007.

[12] J. M. Jin, *The Finite Element Method in Electromagnetics*, John Wiley & Sons, 2002.

[13] J. D. Jackson, *Classical Electrodynamics*, John Wiley & Sons, 1998.

[14] D. Strauss, *Magnetic Drug Targeting in Cancer Therapy*, 2005, http://www.comsol.com/showroom.

[15] R. E. Rosensweig, "An introduction to ferrohydrodynamics," *Chemical Engineering Communications*, vol. 67, no. 1, pp. 1–18, 1988.

[16] R. E. Rosensweig, *Ferrohydrodynamics*, Dover, 1997.

[17] P. A. Voltairas, D. I. Fotiadis, and L. K. Michalis, "Hydrodynamics of magnetic drug targeting," *Journal of Biomechanics*, vol. 35, no. 6, pp. 813–821, 2002.

[18] Y. C. Fung, *Biomechanics: Mechanical Properties of Living Tissues*, Springer, 1993.